HHS Public Access

Author manuscript

Behav Brain Res. Author manuscript; available in PMC 2019 January 30.

Published in final edited form as:

Behav Brain Res. 2018 January 30; 337: 34–45. doi:10.1016/j.bbr.2017.09.026.

Sex-Dependent Behavioral Impairments in the HdhQ350/+ Mouse Line

Jessica K. Cao[1], **Peter J. Detloff**[3], **Richard G. Gardner**[1], and **Nephi Stella**[1,2]

[1]Department of Pharmacology, University of Washington, Seattle, WA 98195

[2]Department of Psychiatry & Behavioral Sciences, University of Washington, Seattle, WA 98195

[3]Department of Biochemistry and Molecular Genetics, University of Alabama at Birmingham, Birmingham, AL 35294

Abstract

Huntington's Disease (HD) is an autosomal dominant neurodegenerative disease characterized by gradual deterioration of motor and cognitive functions and development of psychiatric deficits. Animal models provide powerful means to study the pathological processes, molecular dysfunctions and symptoms associated with HD. We performed a longitudinal behavioral study of the newly developed HdhQ350/+ mouse line, a knock-in model that expresses a repeat of 350 glutamines. We found remarkable sex-dependent differences on symptom onset and severity. While both sexes lose weight and grip strength, only HdhQ350/+ males have impaired motor coordination as measured by the rotarod and alterations in gait as measured by the catwalk assay. While HdhQ350/+ females do not exhibit impairment in motor coordination, we found a reduction in dark phase locomotor activity. Male and female HdhQ350/+ mice do not show anxiety as measured by the elevated plus maze or changes in exploration as measured by the open field test. To investigate these sex-dependent differences, we performed western blot analyses of striatal tissue. We measured equal mutant huntingtin protein expression in both sexes and found evidence of aggregation. We found the expected decrease of DARPP-32 expression only in female HdhQ350/+ mice. Remarkably, we found no evidence of reduction in synaptophysin and CB_1 receptors in HdhQ350/+ tissue of either sex. Our study indicates that male and female HdhQ350/+ mice differentially recapitulate select behavioral impairments commonly measured in other HD mouse models with limited sex-dependent changes in recognized histopathological markers. We conclude that expanded polyglutamine repeats influence HD pathogenesis in a sex-dependent manner.

Correspondence to: Nephi Stella, Department of Pharmacology, University of Washington School of Medicine, Box 357280, Seattle, WA 98195. Tel: (206)221-5220; Fax: (206)543-9520; nstella@uw.edu.

All authors report no conflict of interest.

Keywords

Huntington's Disease; mouse model; sex-dependent; polyglutamine disease; protein aggregation; neurodegeneration

1. Introduction

Huntington's Disease (HD) is a devastating genetic disease caused by an expanded polyglutamine (CAG) tract in exon 1 of the huntingtin gene (*HTT*) located on chromosome 4 [1]. Mutant huntingtin proteins (mHtt) that contain a repeat of more than 35 glutamines aggregate and interfere with the expression and function of thousands of genes and proteins in humans. Within affected brain regions, this interference occurs through several molecular pathways implicated in HD pathogenesis, including sequestration of transcription factors, interference with protein-protein interactions and direct inhibition of enzymes, the combination of which leads to the dysfunction and degeneration of neurons [2, 3]. HD patients exhibit gradual deterioration of motor and cognitive functions and select psychiatric symptoms. The average survival is 15–25 years after initial symptom onset and by end-stage, patients are profoundly demented and debilitated [4]. Currently, there is no cure and available treatments merely address symptoms. Much effort has been dedicated to increasing our understanding of HD pathogenesis and to use this knowledge to develop reliable preclinical models in order to discover novel therapeutics to treat patients diagnosed with HD.

During the past decades, several genetic mouse lines have been developed to model this disease. The first generation rodent models, the R6/1 and R6/2 lines, were developed in the 1990s and are transgenic models that express a truncated form of human *HTT* with a range of 115–150 CAG repeats [5]. The large number of studies performed with R6/1 and R6/2 mice show that these lines do not recapitulate adult-onset HD pathogenesis and present limitations in both pathological and behavioral characteristics of the disease. For example, R6/2 mice exhibit an extremely aggressive and rapid disease progression detected as early as 4–6 weeks of age, a 12–16 week life-span and widespread nuclear mHtt inclusions in brain areas typically unaffected in human HD [6]. R6/2 mice also suffer from a high incidence of symptoms that do not typically develop in human adult-onset HD, including seizures, diabetes and neuromuscular junction abnormalities [7, 8]. Remarkably, studies performed on subsequent R6/2 mouse lines expressing greater than 300 CAG repeats do not exhibit such a rapid disease progression and survive longer than those expressing 115–150 CAG repeats [9]. This may be due to a delayed onset of neuronal mHtt aggregate formation, alteration of accessibility to the nucleus or decreased expression of mRNA [10]. Thus, first generation R6/1 and R6/2 mouse models provided critical insight into the molecular mechanisms involved in HD pathogenesis, including the impact of increasing CAG repeats, setting the foundation for the development of HD mouse models that better recapitulate this neurodegenerative disease.

The next generation mouse models relied on transgenic insertions of full-length human *HTT* containing up to 175 CAG repeats, exhibiting a slower disease progression than their

truncated counterparts and recapitulating many behavioral and neuropathological components of HD pathogenesis. The YAC128 and BACHD models, for example, express full-length *HTT* and exhibit many progressive motor and cognitive behavioral impairments and landmark neuropathological indices in brain areas known to be affected in adult-onset HD [6, 8]. One key variance of the YAC128 and BACHD model systems to human adult-onset HD is the absence of a shortened lifespan. The N171-82Q model expresses a truncated *HTT*, displays motor impairments starting at 12 weeks of age and only live to 24 weeks of age, but does not show pronounced neuronal inclusions in the striatum [8]. The zQ175 model expresses a chimeric human exon 1 carrying expanded CAG repeats inserted into the native murine *huntingtin* gene and homozygous zQ175 mice exhibit early reduced motor and grip strength, as well as a slight reduction in survival of approximately 100 weeks of age [11].

The HdhQ mouse model was developed using gene targeting technology whereby elevated CAG repeats were inserted into the *Hdh* gene, the mouse homolog to the human *HTT* gene [12]. Thus, in contrast to previous HD mouse models, the HdhQ model lacks human DNA and contains a purely murine genome. Natural germline alterations in repeat lengths in the HdhQ150 line were leveraged to create several allelic lines with repeats up to 315 CAGs in length. These lines represent powerful genetic tools to study how changes in the number of CAG repeats affect the pathological process and behavioral impairments in mice and whether they reliably model human adult-onset HD [6]. The heterozygous 200 CAG line (HdhQ200/+) reliably recapitulates key aspects of HD pathology and motor dysfunction, including the accumulation of neuronal mHtt intranuclear inclusions in both the striatum and cortex, as well as mHtt aggregation foci in the cytoplasm after 40 weeks of age. By 80 weeks of age, HdhQ200/+ mice have reduced grip strength and abnormal gait, both of which represent symptoms thought to parallel human HD symptoms [13]. However, HdhQ200/+ mice still live a normal lifespan of approximately 2 years and thus do not mimic the reduced lifespan known to occur in human adult-onset HD. A recent study found that HdhQ315/+ mice had a more aggressive phenotype than the HdhQ200/+ line [10]. HdhQ315/+ mice showed deficits in motor coordination, open field and grip strength as early as 30 weeks of age. Pathologically, HdhQ315/+ mice had striatal aggregates at 70 weeks of age despite not exhibiting neuronal loss. Thus, the HdhQ mouse model represents a reliable genetic tool to study the effects of expanded polyglutamine repeats on disease progression.

Given the altered pathogenesis occurring in the R6 allelic series with elevated CAG repeat lengths, it is still unclear whether HdhQ lines expressing CAGs above 315 repeats will recapitulate the behavioral impairments and neuropathological indices commonly measured in other HD mouse models. Here, we studied a newly developed line of the HdhQ allelic series, mice expressing 350 CAGs, by performing a longitudinal study of behavioral and neuropathological indices commonly measured in other HD mouse models. We found evidence of sex-dependent variances in behavioral impairments with sex-dependent changes in select HD neuropathological indices despite equal expression and aggregation of mHtt in relevant brain areas in animals of each sex.

2. Materials and Methods

2.1. HdhQ350 mice colony

Mice were housed in a pathogenic-free facility in accordance with the National Institutes of Health; the Institutional Animal Care and Use Committee at the University of Washington approved all experiments. All experiments were performed with the HdhQ350 knock-in mouse model, maintained on a C57BL/6 genetic background. For all experiments, female and male heterozygous HdhQ350 knock-in mice were mated to produce heterozygous and wild-type littermates. Both male and female HdhQ350 heterozygous and wild-type mice were used for behavior and pathological analyses. Animals were housed in cages grouped by sex and mixed genotype, had *ad libitum* access to food and water and were on a 12-hour light/dark cycle. Genotyping was performed with tail snips using primers "cccattcattgcccttgctg" and "gcggctgaggggggttga" with a SimpliAmp Thermal Cycler (Thermo Fisher Scientific, Bothell, WA).

2.2. Behavioral studies

Balanced cohorts of males and females were used for behavioral studies. The same individual was analyzed at each time point (every 10 weeks, starting at 30 weeks to 70 weeks of age). All behavioral studies were performed during the light phase of the light/dark cycle, between 9am and 4pm. Cages and equipment were thoroughly cleaned with 70% ethanol and dried with a paper towel between trials. Grip strength was assessed with a grip strength meter (Columbus Instruments, Columbus, OH). With mice grasping a metal grid with their forepaws, continual gentle force was used to pull the mouse slowly away from the grid. A strain gauge recorded the maximum force applied just prior to release. The elevated plus maze was measured with 5-minute trials using a vertically mounted video camera and analyzed in Ethovision XT 9 (Noldus, Wageningen, The Netherlands). With rodents, increased time spent in closed arms denotes increased anxiety and increased time spend in open arms suggests decreased anxiety and more exploration. Rotarod (Med Associates Inc., St. Albans, VT) testing included 7 consecutive trials, separated by 30-minute resting periods over 3 days. The rotarod rotational speed used for testing trails began at 4 rpm and increased to 40 rpm for a maximum of 5 minutes, with an acceleration of 0.2 rpm per every 4 seconds. Motor learning was divided into "fast" and "slow" learning, as adapted from Costa, Cohen [14]. "Fast" motor learning was calculated by the difference between trial 1 and 7 in day 1, and "slow" motor learning was calculated by the difference for all three testing days. Catwalk testing included 3 trials, where animals were placed at one end of the catwalk apparatus (Noldus, Wageningen, The Netherlands), with a vertically mounted camera under the walkway that recorded their movements as they crossed an infrared track. Crossings where the animal stopped, reared or turned around were excluded. The Phenotyper (Noldus, Wageningen, the Netherlands) testing consisted of 72-hour trials where animals were individually housed in 30cm × 30cm Plexiglas cages with access to water, food and housing. A vertically mounted camera continuously tracked animal movement and digital traces were analyzed in Ethovision XT 9.

2.3. Immunohistochemistry

Mice were euthanized with ketamine/xylazine and perfused with 20mL PBS, followed by 10mL 4% paraformaldehyde. Brains were extracted and post-fixed in 4% paraformaldehyde overnight at 4°C. Brains were then dehydrated (first in 15% sucrose and then 30% sucrose for 24 hours each) and frozen over dry ice. Coronal sections were cut to a thickness of 30μm using a sliding microtome and placed in cryoprotectant for storage at −20°C. IHC analysis of each time point group was processed and stained in parallel. For staining, 2 slices per animal were removed from cryoprotectant, washed 3×PBS and incubated for 90 minutes at room temperature in blocking buffer (PBS, 5% goat serum, 1% Triton x-100). Slices were then transferred to primary staining solutions (PBS, 2.5% goat serum, 0.5% Triton x-100) for 72 hours at 4°C. Sections were then washed 8×PBS-T and secondary staining was performed using Alexa secondary antibodies at a dilution of 1:500 (PBS, 2.5% goat serum, 0.5% Triton x-100). Additional slices were stained only with secondary staining solutions to serve as non-specific secondary background staining. After secondary staining, sections were washed 6×PBS-T, 1×PBS, mounted on slides and allowed to dry at room temperature overnight. Coverslips were added and sealed with Fluoromount (Sigma, St. Louis, MO) and nail polish.

2.4. Immunoblotting

Mice were euthanized via cervical dislocation, their brains immediately removed and rinsed in ice cold PBS. Striata were dissected and flash frozen in liquid nitrogen. Striatal tissue was then homogenized in RIPA Buffer (Santa Cruz Biotechnology, Dallas, TX) using a Dounce homogenizer on ice followed by sonication. Protein levels were measured using a BCA assay. Each time point group was processed and analyzed in parallel. Specifically, 20–25μg of protein was loaded per lane and gels were transferred to PVDF and blocked with Licor Odyssey Blocking Buffer (LI-COR, Lincoln, NE). Blots were stained overnight with primary antibodies prepared in TBS solution containing 5% BSA and 0.02% NaN_3 at 4°C, followed by 3 rinses in TBS-T. Secondary staining was carried out for 2 hours in TBS containing 5% BSA at room temperature. Blots were then rinsed 3×TBS-T, imaged and analyzed with fluorescence. Expression level of target proteins was quantified with ImageLab (LI-COR, Lincoln, NE) and normalized to GAPDH expression. Values were normalized to the corresponding wild-type sex average.

2.5. SDDAGE (Semi-Denaturing Detergent Agarose Gel Electrophoresis)

Striatal tissue was prepared as described above and solubilized in SDDAGE lysis buffer (Tris, NaCl, EDTA, 5% glycerol, DTT, 1% NP-40, $MgCl_2$, DNase, PMSF+NEM). Samples were incubated in SDDAGE loading buffer (TAE, 20% glycerol, 8% SDS, 0.01% bromophenol blue) for at least 10 minutes, loaded in a pre-poured gel (TAE, 1.5% agarose, 0.1% SDS) and ran at 34V for 6 hours on ice. Samples were then transferred overnight using a semi-dry capillary apparatus and developed with the western blot protocol described above. Blots were analyzed with HRP.

2.6. Antibodies

The following antibodies were used in this study: CB_1 receptor (L15 pAb guinea pig, gift from Ken Mackie); synaptophysin (mouse, Synaptic Systems 101011); DARPP-32 (rabbit, Abcam ab40801); DAPI (Invitrogen D3571); 1C2 (mouse, Millipore MAB1574); GAPDH (mouse, Sigma 1405848; rabbit, Cell Signaling Technology 5174); Alexa Fluor 488/555/647 (goat/donkey, ThermoFisher); IRDye 680/800 (goat, LI-COR Biosciences); HRP-conjugated secondaries (goat, Cell Signaling Technology).

2.7. Microscopy

Images were collected on a Marianas microscope (Intelligent Imaging Innovations, Inc. Denver, CO) equipped with either 20×/0.75 NA or 40×/0.75 NA air objective lens with CoolSnap HQ cooled monochrome camera (Photometrics, Tucson, AZ) as Z-stacks of 10 at the NIDCD Research Core Center at the University of Washington. Noise reduction of images was achieved by deconvolution of Nearest Neighbors using SlideBook (Intelligent Imaging Innovations, Inc., Denver, CO). Exposure times were optimized for each antibody to ensure that >99% pixels were within the linear range. Excitation laser of 403nm was used to excite DAPI, FITC to excite Alexa 488, Cy3/TRITC to excite Alexa 555, and FarCy5 to excite Alexa 647.

2.8. Semi-quantitative image analysis and statistics

All images were analyzed using ImageJ (National Institutes of Health) with custom written macros. Macros were applied blindly to each batch of images and analyzed as previously reported by our laboratory [15]. Each z-stack was flattened into one image of average pixel intensity and each channel was split into an individual image. The mean intensity and standard deviation of each fluorophore was measured and background signal was removed by thresholding images to mean + standard deviation, corresponding to the top third brightest pixels in the Gaussian distribution. After thresholding, final measurements were made by taking the mean intensity of the remaining pixels or by calculating the average cellular size. Values were normalized to the corresponding wild-type sex average.

2.9. Statistical analyses

Statistical analyses and graphs were generated using GraphPad PRISM 6 (San Diego, CA). Grubbs' test was used to detect any outliers. Two-way ANOVA was used to compare measurements with a Bonferroni post-hoc analysis. A repeated two-way ANOVA was used for behaviors with complete data sets when appropriate. A chi-square test was used for Mendelian frequencies. Data were considered significant if $p<0.05$.

3. Results

3.1. General phenotype of Hdh350/+ mice: Life span, weight and grip strength

Breeding of HdhQ350/+ by HdhQ350/+ mice produced average litter sizes of 4.6 pups. Of 101 mice from this cross, 0 were HdhQ350/350, 44 were HdhQ350/+ and 57 were wild-type, a result which deviates significantly from the normal 1:2:1 expected Mendelian ratio (χ^2 (2, N=3)=64.16, $p<0.0001$). Note that we did not observe any cannibalism after birth

and thus the most likely is that homozygote mice died in utero, and heterozygous HdhQ350 mice show reduced viability.

Up to 70 weeks of age, mice did not exhibit overt signs of tremor, hunching, unsteady movements or staggering gait. We also did not observe any spontaneous or handling-induced seizures [16]. However, by 70 weeks of age, HdhQ350/+ mice of both sexes had significantly reduced weight. Figure 1A shows that HdhQ350/+ males had 9.4% reduced body weight by 40 weeks of age compared to male wild-type littermates, and Figure 1B shows that female HdhQ350/+ mice had 9.2% reduced body weight by 30 weeks of age compared to wild-type littermate females. In addition, post-hoc analyses revealed significant loss as early as 30 weeks of age in female HdhQ350/+ mice. Thus HdhQ350/+ mice of both sexes failed to gain weight as typically seen in wild-type mice. Although there was a significant effect of genotype in both groups (male: $F_{(1, 13)}$=11.23, p=0.005; female: $F_{(1, 14)}$=9.72, p=0.008) (Figure 1A, B), there was no overall effect of sex on weight loss in HdhQ350/+ mice when normalizing weights to wild-type littermates (to assess for progressive weight loss) (Figure 1C). These results show that both male and female HdhQ350/+ mice equally failed to gain weight over time.

Lack of increase in body weight might be due to loss in muscle mass and strength. We used a grip strength meter to measure forelimb grip strength and found that both male and female HdhQ350/+ mice exhibited significantly reduced grip strength compared to respective wild-type littermates when analyzed by two-way ANOVA (male: $F_{(1, 12)}$=7.89, p=0.016; female: $F_{(1, 14)}$=18.39, p=0.001) (Figure 1D, E). Bonferroni post-hoc analysis showed a significant decrease in grip strength in HdhQ350/+ females at 50 weeks of age. Statistical analysis of the reduction in grip strength relative to wild-type mice revealed no sex-dependent loss in HdhQ350/+ mice (Figure 1F). These results suggest that a portion of the reduced body weight mass measured in both male and female HdhQ350/+ mice might be linked to loss of muscle mass.

3.2. Locomotor activity of Hdh350/+ mice: Dark and light phase activities

Several HD mouse models exhibit circadian disturbances typified by increased activity during the night (when mice are active) and decreased activity during the day (when mice are less active) [6, 17]. We used the Noldus PhenoTyper, a home-cage monitoring system, to measure daily patterns of locomotion, hiding, feeding, and drinking over 72-hour time periods. We found that both HdhQ350/+ males and females exhibited an overall decrease in spontaneous locomotion during the active dark phase (male: $F_{(1,61)}$=8.51, p=0.005; female: $F_{(1, 64)}$=45.37, p<0.0001) (Figure 2A, B). Post-hoc analysis indicated that HdhQ350/+ females exhibited a significant decrease in spontaneous activity during the dark phase at 50 weeks of age (Figure 2B). Further analyses between male and female HdhQ350/+ mice when normalized to their respective wild-type littermates to asses for a sex-dependent reduction in dark phase activity revealed an overall significant effect of sex ($F_{(1, 60)}$=15.67, p=0.0002), indicating that female HdhQ350/+ mice were more severely affected (Figure 2C). Post-hoc analysis revealed a significant difference at 70 weeks of age. By sharp contrast, we found no significant differences in spontaneous activity measured during the light phase between HdhQ350/+ mice and their respective wild-type littermates (Figure 2D,

E), and thus, there was no sex-dependent difference in light phase activity in HdhQ350/+ mice (Figure 2F). These results suggest that HdhQ350/+ mice of both sexes exhibited a decrease in spontaneous activity during the dark phase, with females exhibiting a more severe deficit.

To extend these results, we measured the time spent in various zones within the PhenoTyper chamber (i.e. focusing on the time spent along the walls, in the hidden zone, in the feeding zone, and in the drinking zone during the dark phase). We found that HdhQ350/+ mice of both sexes spent similar amounts of time in the hidden zone and feeding zone compared to their respective wild-type littermates (Supplementary Figure 1A–D). We measured significantly increased time spent along the walls of the PhenoTyper chamber for HdhQ350/+ females but not for males, suggesting increased thigmotaxis (tendency for rodents to remain close to vertical surfaces) and possible anxiety ($F_{(1, 60)}$=4.96, p=0.030) (Supplementary Figure 2A, B). In addition, only HdhQ350/+ females spent more time with their bodies contracted, or hunched, at nearly all ages, suggesting possible discomfort and illness ($F_{(1, 60)}$=8.09, p=0.006) (Supplementary Figure 2C, D) [18].

These results demonstrate sex-dependent reduction of nocturnal activity and signs of sickness in HdhQ350/+ mice with overall more pronounced symptoms measured in HdhQ350/+ females. Based on these results, we focused our analysis on 40- and 60-week-old animals, which reflect disease onset and progression in the HdhQ350/+ line, respectively.

3.3. Motor behavior of HdhQ350/+ mice: Motor coordination, motor learning and gait

Motor impairment represents a classical symptom measured in many HD mouse models [3, 6]. Here we determined if HdhQ350/+ mice show deficits in both motor coordination and motor learning as assessed by the accelerating rotarod over 3 days (7 trials per day) [14]. Motor coordination was measured by comparing daily averages of an animal's latency to fall. Figure 3A and C show that at 40 weeks of age, both male and female HdhQ350/+ mice did not differ from wild-type controls in their motor coordination over 3 days of testing. At 60 weeks of age, HdhQ350/+ males showed a significant reduction in motor coordination on the second and third days of testing (day 2: $F_{(1, 14)}$=9.64, p=0.008; day 3: $F_{(1, 13)}$=6.5, p=0.024), whereas HdhQ350/+ females showed no significant reduction in motor coordination (Figure 3A and C). Accordingly, analysis of each group's average latency to fall per age reached significance only in HdhQ350/+ males, especially at 60 weeks of age ($F_{(1, 14)}$=8.54, p=0.011) (Figure 3B, D). These results show that only HdhQ350/+ males reliably recapitulate the common impairment in motor coordination measured in other HD mouse models and that this symptom develops between 40 and 60 weeks of age in the HdhQ350/+ line.

Impaired motor learning is thought to result from dysfunction of the corticostriatal loop involved in the acquisition of new motor skills [3]. To determine the effect of the HdhQ350/+ mutation on motor learning involving the corticostriatal circuitry, we adopted a method developed by Costa, Cohen [14], in which *fast* motor learning is determined by measuring improvement in motor performance on the rotarod within the first training session (day 1) and *slow* motor learning is determined by measuring improvement across all 3

testing days. Figure 4A shows that HdhQ350/+ males exhibited enhanced fast motor learning compared to corresponding wild-type littermates when analyzing data gathered at 40 and 60 weeks of age using a two-way ANOVA ($F_{(1, 14)}$=0.73, p=0.041). Figure 4B shows that HdhQ350/+ females were not significantly different from wild-type females. Analysis between male and female HdhQ350/+ mice normalized to their respective wild-type littermates showed no significant differences between sexes in regards to fast motor learning (Figure 4C). In regards to slow motor learning, we found enhanced slow motor learning in HdhQ350/+ males compared to wild-type males when analyzing data gathered at both 40 and 60 weeks of age ($F_{(1, 14)}$=6.72, p=0.021) (Figure 4D) and again, no difference in females (Figure 4E). Here, post-hoc analysis showed that enhanced slow motor learning reached significance at 40 weeks for HdhQ350/+ males. Further analysis revealed a significant difference between male and female HdhQ350/+ mice in their slow motor learning when normalized to their respective wild-type littermates ($F_{(1, 14)}$=15.11, p=0.0001) (Figure 4F). These results suggest that only HdhQ350/+ male mice exhibit enhanced improvement of motor learning over multiple days of rotarod testing.

Gait abnormalities represent hallmarks of HD symptoms [3]. To complement our measures of motor coordination and learning, we utilized the Noldus CatWalk XT System that allows for unbiased, automated gait analysis. We found a significant reduction in hind paw step cycle (a measurement of the time it takes for a paw to lift and place back down) in female HdhQ350/+ mice ($F_{(1, 40)}$=5.74, p=0.021) but not males (Figure 5A, B). We measured a significant increase in front paw stride length in HdhQ350/+ males ($F_{(1, 42)}$=4.59, p=0.038) but not in HdhQ350/+ females when compared to their respective wild-type littermates (Figure 5C, D) and no differences in front paw or hind paw swing speed for either sex (Supplementary Figure 3A–D). There was a significant difference in front paw base of support in HdhQ350/+ males but not females, as these mice had a reduced base of support, indicative of reduced stability through movement ($F_{(1, 19)}$=5.35, p=0.032) (Figure 5E, F). Bonferroni post-hoc tests reached significance at 60 weeks of age in HdhQ350/+ males (Figure 5E). Together, these results suggest that HdhQ350/+ mice, especially males, show clear gait abnormalities and that part of the changes in their motor performance as measured by the spontaneous locomotion and motor coordination and learning could be accounted for by changes in gait.

3.4. Psychiatric and cognitive function of HdhQ350/+ mice: Anxiety and exploration

HD patients exhibit a spectrum of psychiatric symptoms that range from irritability to psychosis and include anxiety and loss of interest [3, 6]. Indices of anxiety can be measured in mice with the elevated plus maze and when coupled to measures of novel environment exploration, provide an initial assessment of psychiatric and cognitive dysfunction. Analysis of anxiety using the elevated plus maze confirmed that male and female wild-type mice spent more time in the closed arms than the open arms of the maze (Figure 6A–D). When comparing HdhQ350/+ to wild-type mice, we found no significant differences in the time spent in the closed or open arms irrespective of age or sex (Figure 6A–D). Furthermore, we found no change in the frequency to enter the closed arms for either sex but did find a significant difference in the frequency to enter open arms for female HdhQ350/+ mice

($F_{(1, 13)}$=5.78, p=0.032), but not for male mice (Supplementary Figure 4A–D). These results show that HdhQ350/+ mice do not exhibit overt changes in anxiety.

Activity in the first hour of being placed in the PhenoTyper chamber was used to assess the mouse's interest and exploratory behavior of a novel environment. As expected, male and female wild-type mice showed high levels of exploration activity during the initial hour, covering approximately 100 meters/hour compared to approximately 10 meters/hour when measured 24 hours later (Figure 6E, F and Supplementary Figure 5A, B). There was no difference between male and female HdhQ350/+ and wild-type littermates in their exploratory activity during this initial hour when measured at 40 or 60 weeks of age (Figure 6E, F). Expectedly, we found no difference in activity 24 hours later between HdhQ350/+ and wild-type male mice (Supplementary Figure 5A). Curiously, we found a significant increase in activity 24 hours later in HdhQ350/+ females over wild-type females, especially at 60 weeks of age ($F_{(1, 27)}$=6.77, p=0.015) (Supplementary Figure 5B). Taken together, these results suggest no striking anxiety or reduction in exploratory behavior exhibited by the HdhQ350/+ mouse line.

3.5. mHtt expression in HdhQ350/+ brains: Protein expression and aggregation

A portion of HD pathogenesis is linked to mHtt aggregates accumulating in the striatum [3, 19]. To verify that mHtt protein is expressed and aggregates in HdhQ350/+ striatum, we measured mHtt expression in this tissue by western blot using an antibody that recognizes polyglutamine expansions over 37 CAGs [20]. Supplementary Figure 6A and B show that mHtt protein is expressed in the striatum of both male and female HdhQ350/+ mice and as expected, aggregates were detected in the stacking gel. Aggregated Htt was not observed in wild-type littermates. Furthermore, mHtt proteins expressed by male and female HdhQ350/+ ran at similar sizes and semi-quantitative analysis of the band intensity indicated no significant difference in expression levels between sexes at 40 or 60 weeks of age (Figure 7A). Analyses of mHtt expression between 40 and 60 weeks revealed no significant differences for either sex (data not shown). These results show that mHtt protein is expressed at similar levels in both male and female HdhQ350/+ striatum.

To extend these results, we used semi-denaturing detergent agarose gel electrophoresis (SDDAGE) to detect large polymers formed by mHtt proteins [21]. This approach has been successfully used to study the aggregation of proteins with elevated polyglutamine repeats. Accordingly, we validated this method using stringent standards of the field: a yeast model expressing 25 polyglutamines as a negative control and a yeast model expressing 103 polyglutamines and Rnq1, a yeast prion known to also form amyloid aggregates, as positive controls [22]. Thus, under low SDS conditions and blotting with an antibody that recognizes large polyglutamine tracts, we found a clear signal indicating aggregates in striatal HdhQ350/+ tissue (Figure 7B). Together, these results demonstrate the equal expression and aggregation of HdhQ350 protein in the striatum of male and female HdhQ350/+ mice.

3.6. Neuropathology of HdhQ350/+ brains: Medium spiny neurons and neuronal markers

To investigate whether motor behavior impairments measured in the HdhQ350/+ model might be correlated with known neuropathological markers of HD pathogenesis, we used

western blots and semi-quantitative immunohistochemistry (sqIHC) to assess for the expression of DARPP-32, synaptophysin and CB_1 receptors in the striatum as previously described by our laboratory [15]. We first measured the expression of DARPP-32, a dopamine- and cAMP-regulated neuronal phosphoprotein in medium spiny neurons (MSNs) known to be down-regulated in mouse models of HD [2], and found a significant reduction in its expression in female HdhQ350/+ mice at 40 and 60 weeks when compared to female wild-type littermates ($F_{(1, 4)}$=47.38, p=0.002) and no change in HdhQ350/+ males compared to male wild-type littermates (Figure 8A, B). To investigate if this difference was due to a reduction of DARPP-32-specific protein expression or general cell loss, we used sqIHC analysis on brain slices that focused on the dorsal lateral striatum. We assessed for cell loss by measuring the size of DARPP-32-positive cells and found no significant difference between genotypes in either sex (Figure 8C, D). Analyzing the number of DAPI-positive cells further validated this result, as we found no differences between genotypes, irrespective of sex (Figure 8E, F). These results suggest that only female HdhQ350/+ mice show a reduction in striatal DARPP-32 expression with no evidence of cell loss.

Loss in the expression of both synaptophysin, a key component of presynaptic machinery for neurotransmitter release, and the cannabinoid CB_1 receptor, a presynaptic G protein-coupled receptor that regulates neurotransmitter release, represent neuropathological hallmarks of early HD pathogenesis [23, 24]. Western blot analysis of striatal tissue showed no difference in synaptophysin expression in male or female HdhQ350/+ mice and wild-type littermates, irrespective of age (Supplementary Figure 7A, B). Reduction of CB_1 receptor expression is known to occur in MSNs of several HD mouse models [15, 25–27]. Interestingly, we found no significant changes in CB_1 receptor expression in the striatum with this mouse model (Supplementary Figure 7C, D). Using sqIHC, we then investigated CB_1 expression on the MSN terminals projecting into the globus pallidus by co-staining with enkephalin and also found no changes in CB_1 expression on the axon terminals (Supplementary Figure 8A, B). Combined, these results show that the expression of certain neuropathological markers of HD pathogenesis (DARPP-32) is reduced in the HdhQ350/+ mouse model in a sex-dependent manner.

4. Discussion

We report a longitudinal study of the HdhQ350/+ mouse line that focuses on behavioral indices commonly measured in other mouse models of HD. We provide evidence for sex-dependent alterations of motor performance as measured by several readouts and no evidence of anxiety or decreases in exploratory behavior. HdhQ350/+ mice had reduced weight and grip strength independent of sex. While we demonstrate that the HdhQ350 protein is expressed and aggregated in the brain, we only found a significant decrease in DARPP-32 expression in female HdhQ350/+ mice, with no significant changes in the expression of two other neuropathological markers commonly measured in HD research. Our study indicates that the HdhQ350/+ mouse line recapitulates select physical and behavioral impairments commonly measured in other HD mouse models but not equal loss of common neuropathological markers. In addition, our results suggest that polyglutamine expansions and expression of mHtt protein may affect disease progression and severity in a

sex-dependent manner, indicating an importance to study both sexes with other HD and polyglutamine animal models.

The HdhQ350/+ mouse line was generated through selective breeding of the HdhQ mouse model. Here we report that, unlike the HdhQ150 and HdhQ200 lines, homozygous HdhQ350/350 mice were most likely embryonic lethal [13, 28]. This has been previously noted to occur in the HdhQ315/+ line [10]. In addition, we found a significant reduction in heterozygote viability. The HdhQ350 line does reproduce several key physical symptoms known to occur in other HD mouse models. We show that HdhQ350/+ males and females exhibit significant weight loss as early as 30 weeks of age, whereas it has been published that only female HdhQ200/+ mice lose weight after 50 weeks of age and HdhQ150/+ mice do not display any weight deficits [13]. Because mice spent normal amounts of time at the feeding area of the PhenoTyper cage and no overt deficits in feeding behavior were observed by researchers and animal technicians, this weight loss is likely due to a physiological impairment that remains to be identified. Interestingly, the early loss in weight is paralleled by a reduction in grip strength; both male and female HdhQ350/+ mice exhibit reduced forelimb grip strength at 30 weeks of age. This result contrasts with what has been measured in HdhQ200/+ mice, which do not exhibit this phenotype until 80 weeks of age [13]. While early reduction in grip strength suggests that the HdhQ350/+ mice may have a defect in muscle development, a study of muscle tissue is needed to better understand this HdhQ350/+ associated impairment.

We found significant changes in dark phase spontaneous activity in both HdhQ350/+ males and females and no changes in light phase activity. Remarkably, we found a more severe phenotype in female HdhQ350/+ mice, especially at 70 weeks of age. A study on circadian patterns with the R6/2 model showed shifted circadian patterns and there has been evidence of phase-delayed circadian rhythm in HD patients [17, 29]. Together, these results suggest that HdhQ350/+ mice exhibit similar activity disturbances to other mouse models of HD.

Analysis of motor coordination using the rotarod revealed significant deficits at 60 weeks of age in male HdhQ350/+ mice. Both HdhQ150/+ and HdhQ200/+ mice do not exhibit motor deficits on the rotarod and even HdhQ150/150 mice do not show a deficit until 100 weeks of age [13, 28]. In line with our results, a study on BACHD mice revealed that male BACHD mice exhibit poorer motor coordination than female BACHD mice [30]. In addition, a study on a transgenic HD rat model showed motor impairments in only males and a study on R6/2 mice showed that males exhibited earlier symptoms of other motor impairments, including hanging, rearing and climbing [31, 32]. Analysis of wheel-running, another measurement of motor activity, on R6/1 mice also showed a decrease only in males [33]. Furthermore, we found striking differences in motor learning with male HdhQ350/+ mice, suggesting disruptions or adaptations in the corticostriatal loop in this mouse line. The corticostriatal loop is involved in action selection, motor control, sequence learning, and habit formation [34]. However, we also note that our results may be due to the initial poorer starting performance of the HdhQ350/+ mice and/or impairment of learning retention between days, either of which would result in a poorer initial performance of the first trial for HdhQ350/+ animals in the rotarod assay. In any case, this represents a novel finding, as motor learning has not been explored in-depth in previous HD mouse models.

Earlier studies have reported gait instability in the HdhQ150/150, HdhQ150/+, HdhQ200/+, and HdhQ315/+ lines, as measured by different paradigms than in our study. Specifically, 70-week-old HdhQ150/150 and 50-week-old HdhQ200/+ mice are significantly unstable when traversing a balance beam [10, 13, 28]. In addition, HdhQ315/+ animals show a slower latency to traverse a ladder starting at 40 weeks of age as well [10]. The Noldus CatWalk XT System used in our study is an automated, highly sensitive tool that detected slight alterations mainly in male HdhQ350/+ mice. Specifically, we saw increases in the length of stride of their front paws and decreases in their front base of support. Thus, sex-dependent gait instability occurs in the HdhQ350/+ line.

Psychiatric deficits and cognitive dysfunction as measured by indices of anxiety and exploration have not been studied in previous HdhQ lines, and our study uncovered no significant impairments in these behavioral readouts. Whereas we saw initial indication of anxiety through thigmotaxis in the PhenoTyper chamber in female HdhQ350/+ mice, this impairment was not confirmed with the elevated plus maze. Note that studies have shown that only female R6/1 mice exhibit depressive-like phenotypes, as measured with the sucrose preference test, forced swim test, tail-suspension test, and novelty-suppressed feeding test [6], which may be linked to a disruption in the hypothalamic-pituitary-adrenal axis [35]. These mice also have disrupted short-term memory acquisition due to stress, suggesting sex-dependent cognitive deficits [36]. By contrast, R6/2 and BACHD mice exhibit decreased anxiety as measured by the elevated plus maze, and a study on R6/2 and HdhQ mice carrying increasing CAG repeats showed a nonlinear profile of depression through the forced swim test [37–39]. It is important to emphasize that psychiatric deficits may depend on the behavioral paradigm and readout, as select HD mouse models exhibit differing results with the open field test, elevated Z maze, fear conditioning, and forced swim test [6]. Based on this evidence, we conclude that there may be sex-dependent psychiatric deficits that are detected using certain behavioral paradigms.

One of the most interesting findings of our analyses is a sex difference in the disease progression occurring in the HdhQ350 line. Few studies on other HD mouse models have separately analyzed male and female cohorts and previous studies on HdhQ150, HdhQ200 and HdhQ315 lines did not identify any overt sex-differences [10, 13, 28]. We found a more severe general phenotype in HdhQ350/+ females with an earlier onset of weight loss, increased body contractions indicating distress, increased thigmotaxis and a more severe loss of dark-phase locomotor activity. Conversely, we measured a more severe impairment in motor coordination and learning, as well as gait in HdhQ350/+ males. Taken together, our results suggest possible sex-dependent behavioral deficits due to the HdhQ350/+ mutation.

We show that the HdhQ350 line also models a sex-dependent reduction of striatal DARPP-32 expression only in HdhQ350/+ females. Interestingly, heterozygous and homozygous HdhQ150 mice of both sexes show significant reduction in the number of MSNs by 100 weeks of age whereas this does not occur in HdhQ200/+, HdhQ315/+ or in our HdhQ350/+ mice. These previous studies did not report any sex differences. Combined with our results, this suggests that the elevated CAG repeats may differentially affect sexes in mouse models [13, 28]. Our results propose that the behavioral symptoms we measured in the HdhQ350 line results from dysfunction rather than loss of striatal neurons. Remarkably,

we did not detect a down-regulation of synaptophysin or CB_1 receptor expression, common markers of HD pathogenesis. While downregulation of these two markers has been demonstrated in most HD mouse models, no evidence exists for their direct involvement in disease development [15, 25, 40, 41]. In fact, our laboratory showed that despite genetically restoring expression of CB_1 receptors in MSNs of R6/2 mice, motor impairments were not rescued [25]. Thus, further investigation into other synaptic markers would be needed to identify the neuronal dysfunctions occurring in the HdhQ350/+ model.

R6/2 mice carrying over 200 CAG repeats show a delayed onset of symptoms and prolonged survival than those expressing under 200 CAG repeats [9]. Importantly, this incidence does not parallel what is observed in human HD patients, where disease severity strongly correlates with the number of CAG repeats in a patient's gene [42]. When assessing disease onset and progression in the HdhQ150/+, HdhQ200/+, HdhQ315/+ and our current study on the HdhQ350/+ mouse lines [10, 13, 28], it appears that increasing the number of CAG repeats to 350 may elicit molecular mechanisms of neuronal dysfunction that differ from previously developed mouse models of HD [43] and may recapitulate on a portion of human HD.

In summary, we show that the HdhQ350/+ mouse line expresses mHtt proteins that aggregate. We expected parallel declines in behavioral measurements and neuropathology indices in both male and female HdhQ350/+ mice, hypothesizing that key HD markers would decline prior to symptom onset. However, the discrepancies between our neuropathological and behavioral measures revealed a clear disassociation between the development of pathology and behavior in this mouse line. In addition, we found differences in disease onset and severity between males and females. We conclude that elevated CAG repeats trigger sex-dependent pathological processes that remain to be identified, indicating an importance of considering sex when studying HD animal models.

Supplementary Material

Refer to Web version on PubMed Central for supplementary material.

Acknowledgments

The CHDD Behavioral Core and Dr. Toby Cole for advising and providing access to behavioral equipment. The CHDD Microscopy Center and Dr. Glen MacDonald for advising and providing access to the Marianas Live Cell Imaging Microscope. Sofia Simonton Siegel for assistance with experiments. Dr. Gwenn Garden and Dr. John Neumaier for advising on this study and manuscript. The work was supported by National Institutes of Health DA026430 to NS and GM114112 to RG.

References

1. MacDonald, ME., et al. Cell. Elsevier; 1993. A novel gene containing a trinucleotide repeat that is expanded and unstable on Huntington's disease chromosomes; p. 971-983.
2. Roze, E., et al. Frontiers in neuroanatomy. Frontiers Media SA; 2011. Huntington's disease and striatal signaling.
3. Walker, FO. Lancet. Elsevier; 2007. Huntington's disease; p. 218-228.
4. Ross, CA., Tabrizi, SJ. The Lancet Neurology. Elsevier; 2011. Huntington's disease: from molecular pathogenesis to clinical treatment; p. 83-98.

5. Mangiarini L, et al. Exon 1 of the HD gene with an expanded CAG repeat is sufficient to cause a progressive neurological phenotype in transgenic mice. Cell. 1996:493–506. [PubMed: 8898202]
6. Pouladi MA, Morton AJ, Hayden MR. Choosing an animal model for the study of Huntington's disease. Nat Rev Neurosci. 2013:708–721. [PubMed: 24052178]
7. Woodman B, et al. The HdhQ150/Q150 knock-in mouse model of HD and the R6/2 exon 1 model develop comparable and widespread molecular phenotypes. Brain Research Bulletin. 2007:83–97.
8. Heng MY, Detloff PJ, Albin RL. Rodent genetic models of Huntington disease. Neuroscience. 2008:1–9.
9. Morton AJ, et al. Paradoxical delay in the onset of disease caused by superlong CAG repeat expansions in R6/2 mice. Neuroscience. 2009:331–341. [PubMed: 19358880]
10. Kumar, A., et al. Human Molecular Genetics. Oxford University Press; 2016. Allelic Series of Huntington's Disease Knock-in Mice Reveals Expression Discorrelates; p. ddw040
11. Menalled LB, et al. Comprehensive Behavioral and Molecular Characterization of a New Knock-In Mouse Model of Huntington's Disease: zQ175. PLoS ONE. 2012:e49838. [PubMed: 23284626]
12. Lin, C-H., et al. Human Molecular Genetics. Oxford Univ Press; 2001. Neurological abnormalities in a knock-in mouse model of Huntington's disease; p. 137-144.
13. Heng MY, et al. Early autophagic response in a novel knock-in model of Huntington disease. Human Molecular Genetics. 2010:3702–3720. [PubMed: 20616151]
14. Costa RM, Cohen D, Nicolelis MAL. Differential Corticostriatal Plasticity during Fast and Slow Motor Skill Learning in Mice. Current Biology. 2004:1124–1134. [PubMed: 15242609]
15. Horne EA, et al. Downregulation of cannabinoid receptor 1 from neuropeptide Y interneurons in the basal ganglia of patients with Huntington's disease and mouse models. Eur J Neurosci. 2012:429–440. [PubMed: 23167744]
16. Naydenov, AV., et al. Neuron. Elsevier Inc.; 2014. ABHD6 Blockade Exerts Antiepileptic Activity in PTZ-Induced Seizures and in Spontaneous Seizures in R6/2 Mice; p. 361-371.
17. Morton, AJ. Experimental Neurology. Elsevier Inc.; 2013. Circadian and sleep disorder in Huntington's disease; p. 34-44.
18. Horn, CC., et al. Front Neurosci. Frontiers; 2011. Behavioral patterns associated with chemotherapy-induced emesis: a potential signature for nausea in musk shrews; p. 88
19. Labbadia J, Morimoto RI. Huntington's disease: underlying molecular mechanisms and emerging concepts. Trends Biochem. Sci. 2013:378–385. [PubMed: 23768628]
20. Trottier Y, et al. Polyglutamine expansion as a pathological epitope in Huntington's disease and four dominant cerebellar ataxias. Nature. 1995:403–406.
21. Halfmann R, Lindquist S. Screening for amyloid aggregation by Semi- Denaturing Detergent-Agarose Gel Electrophoresis. J Vis Exp. 2008
22. Konopka CA, Locke MN, Gallagher PS. A yeast model for polyalanine-expansion aggregation and toxicity. Molecular biology of …. 2011
23. Goto S, Hirano A. Synaptophysin expression in the striatum in Huntington's disease. Acta Neuropathol. 1990:88–91. [PubMed: 2141751]
24. Glass M, Faull RL, Dragunow M. Loss of cannabinoid receptors in the substantia nigra in Huntington's disease. NSC. 1993:523–527.
25. Naydenov, AV., et al. Neuroscience. Elsevier Inc.; 2014. Genetic rescue of CB1 receptors on medium spiny neurons prevents loss of excitatory striatal synapses but not motor impairment in HD mice; p. 140-150.
26. Denovan-Wright EM, Robertson HA. Cannabinoid receptor messenger RNA levels decrease in a subset of neurons of the lateral striatum, cortex and hippocampus of transgenic Huntington's disease mice. NSC. 2000:705–713.
27. McCaw EA, et al. Structure, expression and regulation of the cannabinoid receptor gene (CB1) in Huntington's disease transgenic mice. Eur J Biochem. 2004:4909–4920. [PubMed: 15606779]
28. Heng MY, et al. Longitudinal Evaluation of the Hdh(CAG)150 Knock-In Murine Model of Huntington's Disease. Journal of Neuroscience. 2007:8989–8998. [PubMed: 17715336]

29. Morton AJ, et al. Disintegration of the sleep-wake cycle and circadian timing in Huntington's disease. Journal of Neuroscience. 2005:157–163. [PubMed: 15634777]
30. Kuljis DA, et al. Sex Differences in Circadian Dysfunction in the BACHD Mouse Model of Huntington's Disease. PLoS ONE. 2016:e0147583. [PubMed: 26871695]
31. Bode FJ, et al. Sex differences in a transgenic rat model of Huntington's disease: decreased 17-estradiol levels correlate with reduced numbers of DARPP32+ neurons in males. Human Molecular Genetics. 2008:2595–2609. [PubMed: 18502785]
32. Zarringhalam K, et al. An open system for automatic home-cage behavioral analysis and its application to male and female mouse models of Huntington's disease. Behavioural Brain Research. 2012:216–225. [PubMed: 22266926]
33. Zajac MS, et al. Wheel running and environmental enrichment differentially modify exon-specific BDNF expression in the hippocampus of wild-type and pre-motor symptomatic male and female Huntington's disease mice. Hippocampus. 2010:621–636. [PubMed: 19499586]
34. Shepherd, GMG. Corticostriatal connectivity and its role in disease. Nature Publishing Group; 2013. p. 1-14.
35. Du X, et al. Environmental enrichment rescues female-specific hyperactivity of the hypothalamic-pituitary-adrenal axis in a model of Huntington's disease. Transl Psychiatry. 2012:e133. [PubMed: 22760557]
36. Mo C, et al. Short-term memory acquisition in female Huntington's disease mice is vulnerable to acute stress. Behavioural Brain Research. 2013:318–322.
37. Adjeroud N, et al. Reduced impact of emotion on choice behavior in presymptomatic BACHD rats, a transgenic rodent model for Huntington Disease. Neurobiol Learn Mem. 2015
38. Bissonnette S, et al. Striatal pre-enkephalin overexpression improves Huntington's disease symptoms in the R6/2 mouse model of Huntington's disease. PLoS ONE. 2013:e75099. [PubMed: 24040390]
39. Ciamei, A., Detloff, PJ., Morton, AJ. Behavioural Brain Research. Elsevier B.V.; 2015. Progression of behavioural despair in R6/2 and Hdh knock-in mouse models recapitulates depression in Huntington's disease; p. 1-7.
40. Blazquez C, et al. Loss of striatal type 1 cannabinoid receptors is a key pathogenic factor in Huntington's disease. Brain. 2010:119–136. [PubMed: 20929960]
41. Dowie, MJ., et al. NSC. Elsevier Inc.; 2009. Altered CB1 receptor and endocannabinoid levels precede motor symptom onset in a transgenic mouse model of Huntington's disease; p. 456-465.
42. Andrew SE, et al. The relationship between trinucleotide (CAG) repeat length and clinical features of Huntington's disease. Nat. Genet. 1993:398–403. [PubMed: 8401589]
43. Duzdevich D, et al. Unusual structures are present in DNA fragments containing super-long Huntingtin CAG repeats. PLoS ONE. 2011:e17119. [PubMed: 21347256]

Highlights

- The first characterization of the HdhQ350/+ mouse line.
- HdhQ350/+ mice exhibit sex-dependent behavioral motor impairments.
- HdhQ350/+ mice express mutant huntingtin protein and aggregation.
- HdhQ350/+ mice exhibit sex-dependent changes in select neuropathological indices of Huntington's Disease.
- Elevated polyglutamine expansions may cause sex-dependent behavioral impairments and changes in neuropathological indices.

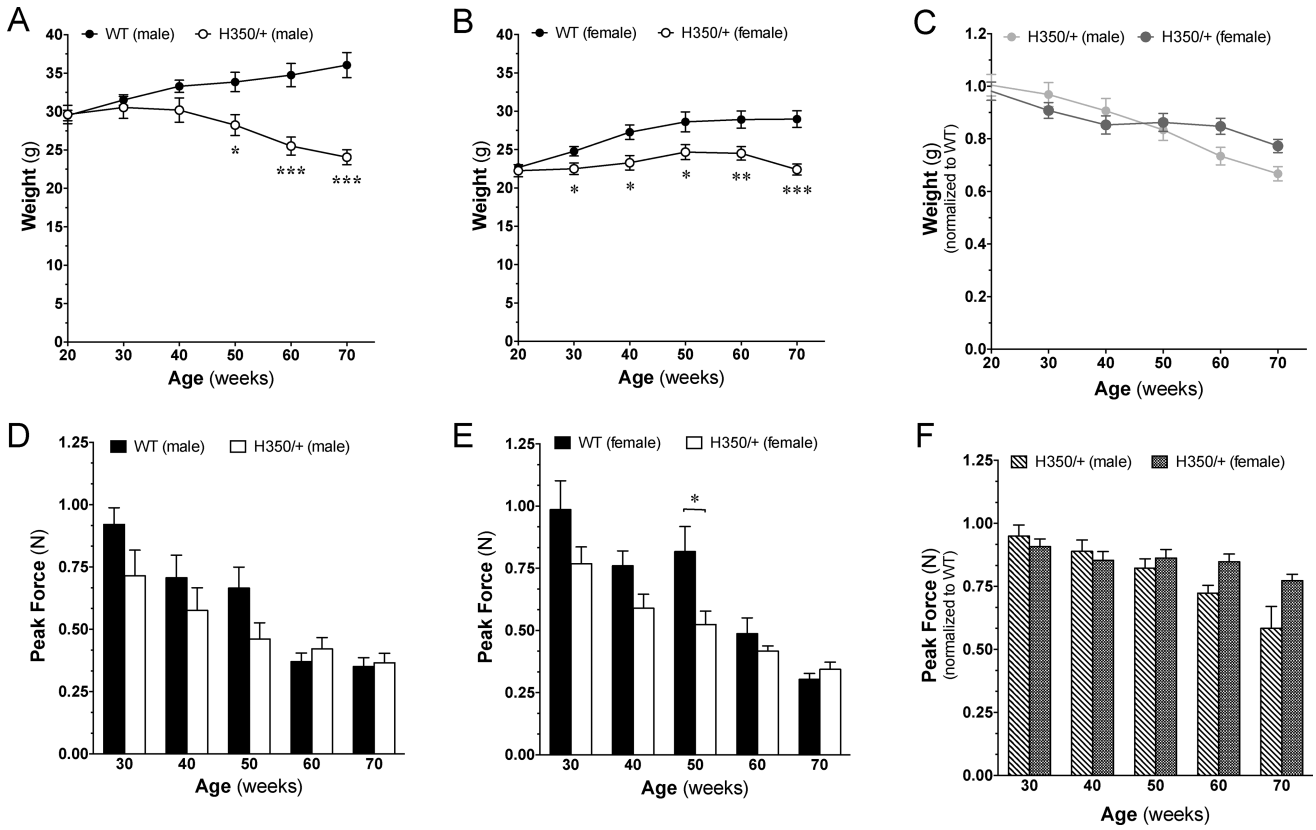

Figure 1. General phenotype of HdhQ350/+ male and female mice compared to wild-type littermates

(A) Male and (B) female HdhQ350/+ mice showed reduced weight compared to their respective wild-type littermates. (C) When normalized to their respective wild-type littermates, both male and female HdhQ350/+ had similar reductions in weight. (D) Male and (E) female HdhQ350/+ mice showed reduced grip strength, starting at 30 weeks of age. (F) When normalized to their respective wild-type littermates, both sexes had similar reductions in grip strength. N=7–8 for all groups. Error bars represent S.E.M. and *p<0.05, **p<0.01, ***p<0.001 with two-way ANOVA with Bonferroni post-hoc test.

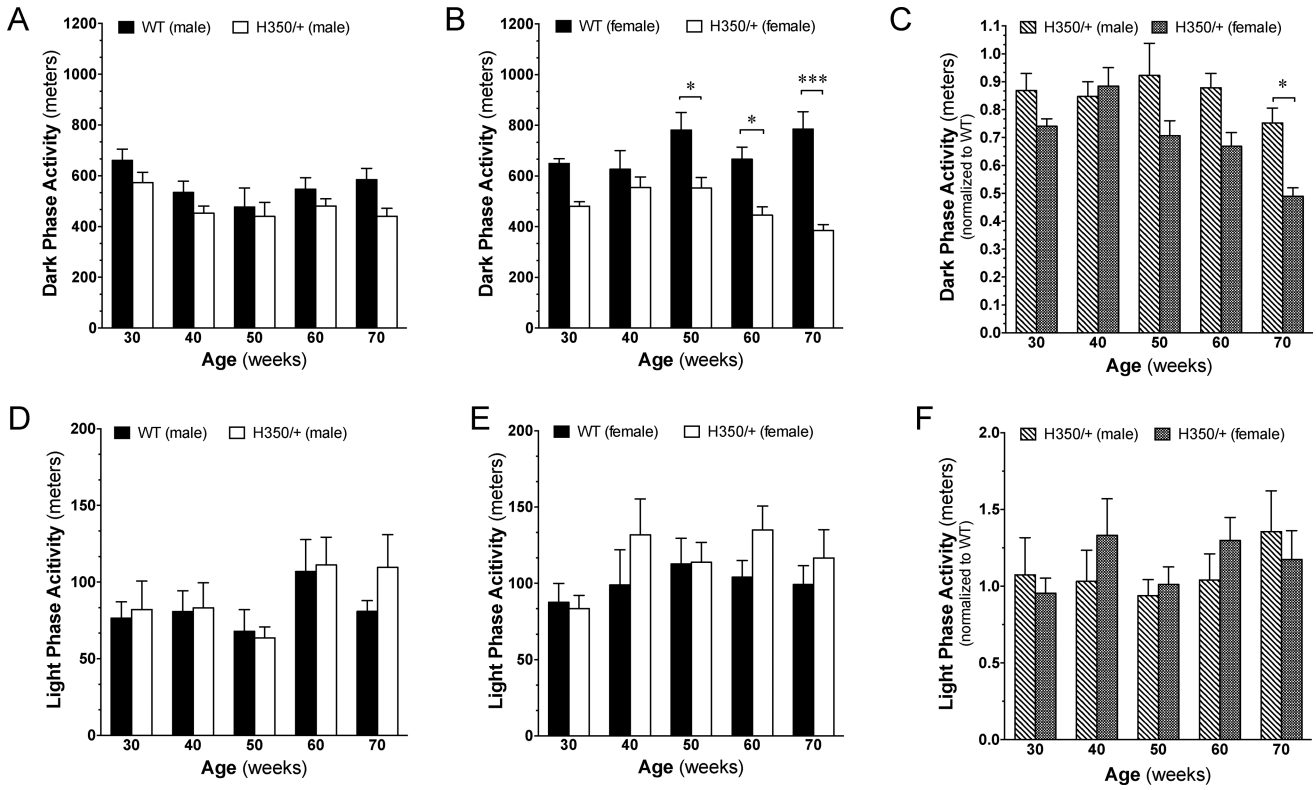

Figure 2. Spontaneous locomotor activity is affected in the dark, but not light, phase

(A) Male and (B) female HdhQ350/+ mice traveled less during the dark phase compared to their respective wild-type littermates. (C) Female HdhQ350/+ mice showed a sex-dependent decline in locomotor activity during the dark phase when normalized to their respective wild-type littermates. (D) Male and (E) female HdhQ350/+ mice traveled similarly to their respective wild-type littermates during the light phase. (F) There was no sex-dependent difference in locomotor activity during the light phase when normalized to their respective wild-type littermates. N=7–8 for all groups. Error bars represent S.E.M. and *p<0.05, ***p<0.001 with two-way ANOVA with Bonferroni post-hoc test.

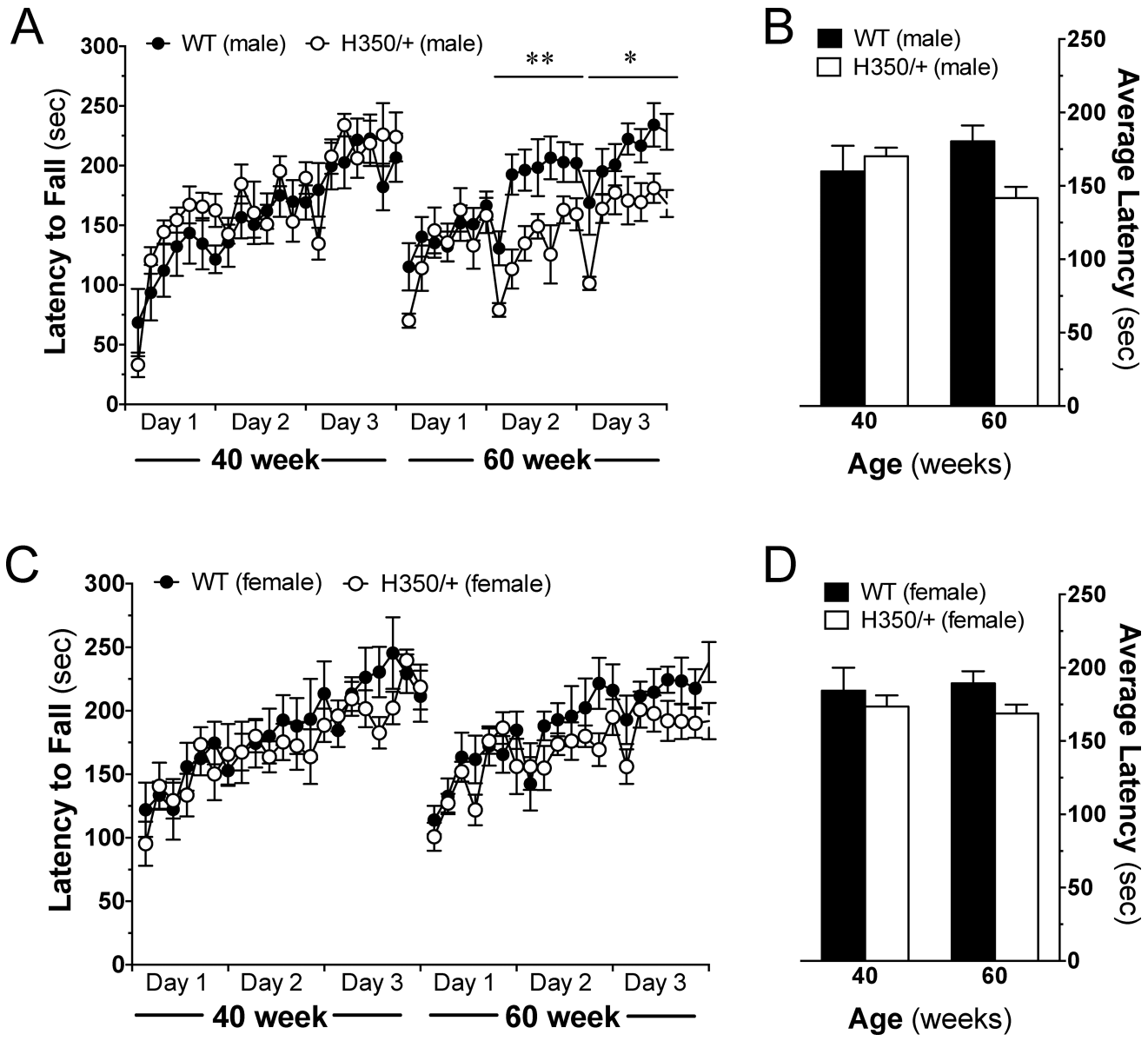

Figure 3. Motor coordination is affected in male, but not female, HdhQ350/+ mice

Mice were tested over 3 days on an accelerating rotarod at various ages. (A) Male HdhQ350/+ mice showed reduced motor coordination on the second and third trial days at 60 weeks of age. (B) Male HdhQ350/+ mice had a lower average latency to fall at 60 weeks of age. (C) Female HdhQ350/+ mice had similar motor coordination on all trial days, compared to female wild-type littermates. (D) Female HdhQ350/+ mice had similar average latencies to fall at 40 and 60 weeks of age. N=7–8 for all groups. Error bars represent S.E.M. and *$p<0.05$, **$p<0.01$ with two-way ANOVA with Bonferroni post-hoc test.

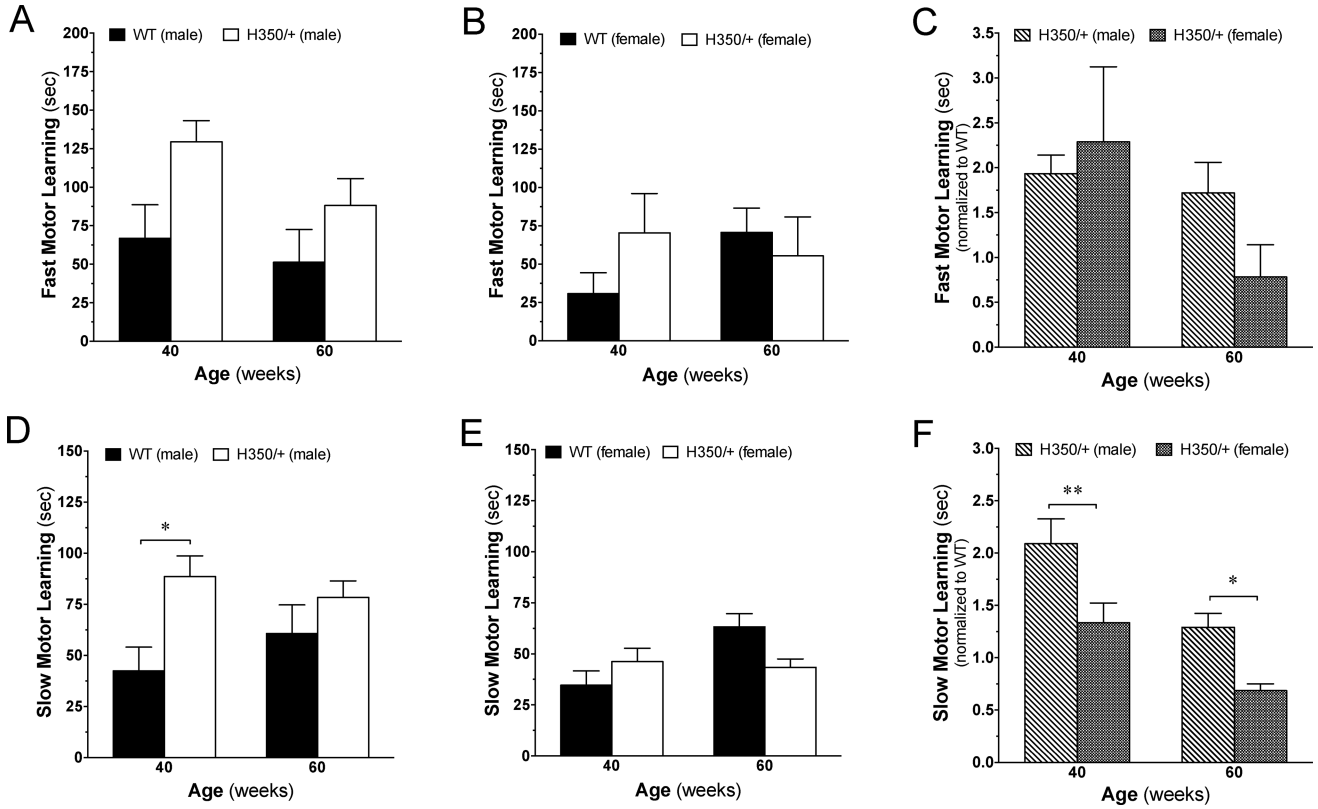

Figure 4. Motor learning is affected in male, but not female, HdhQ350/+ mice

Fast motor learning was calculated by improved performance between the first and last trial on day 1. Slow motor learning was calculated by cumulative improved performance over all 3 days (See Materials and Methods). (A) HdhQ350/+ males showed significantly enhanced fast motor learning while (B) HdhQ350/+ females did not. (C) Comparison of male HdhQ350/+ mice to female HdhQ350/+ mice when normalized to their respective wild-type littermates in fast motor learning revealed no difference between sexes. (D) HdhQ350/+ males showed significantly enhanced slow motor learning while (E) HdhQ350/+ females did not differ from their respective wild-type littermates. (F) Comparison of male HdhQ350/+ mice to female HdhQ350/+ mice when normalized to their respective wild-type littermates revealed a significant difference in slow motor learning between sexes. N=8 for all groups. Error bars represent S.E.M. and *p<0.05, **p<0.01, with two-way ANOVA with Bonferroni post-hoc test.

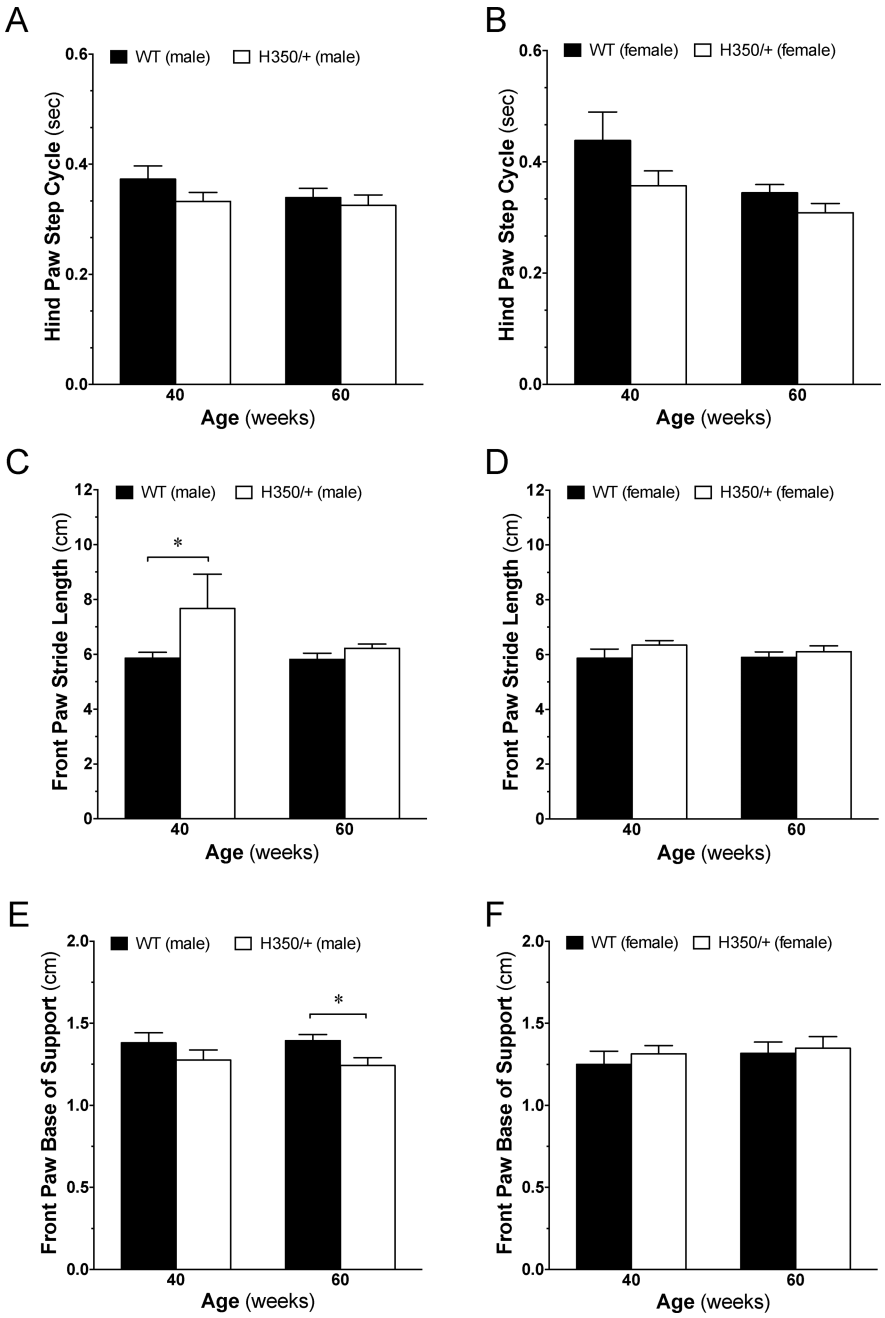

Figure 5. HdhQ350/+ males and females show deficits in gait

(A) Male HdhQ350/+ mice do not have altered hind paw step cycle but (B) female HdhQ350/+ show increased hind paw step cycle at 40 and 60 weeks of age. (C) Male HdhQ350/+ mice have increased front paw stride length at 40 and 60 weeks of age but (D) female HdhQ350/+ mice do not. (E) Male HdhQ350/+ mice have reduced front paw base of support but (F) female HdhQ350/+ mice do not. N=6–8 for all groups. Error bars represent S.E.M. and *p<0.05, with two-way ANOVA with Bonferroni post-hoc test.

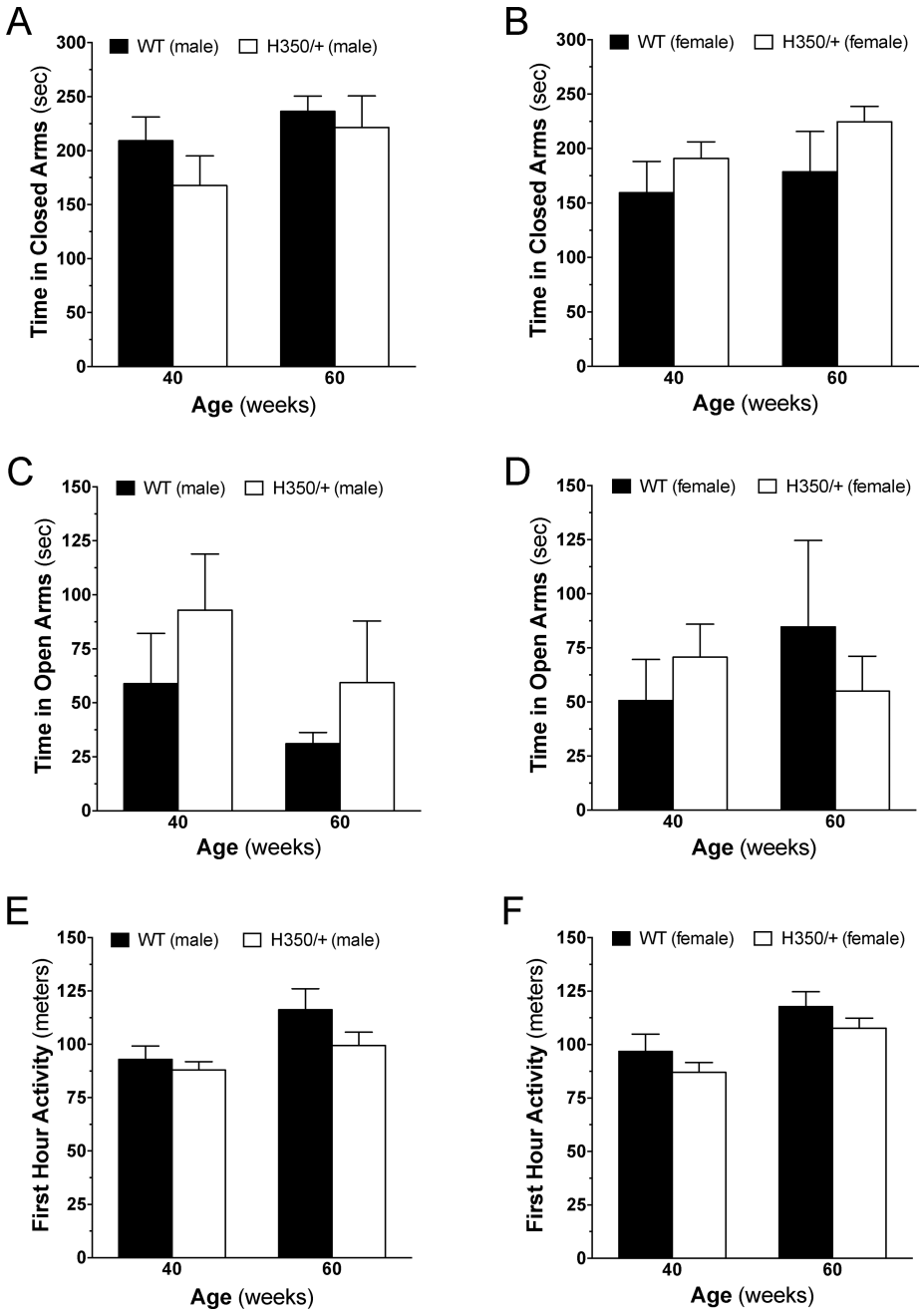

Figure 6. Psychiatric and cognitive functions are unaffected in HdhQ350/+ males and females

On the elevated plus maze, HdhQ350/+ (A) males and (B) females generally spent similar amounts of time in the closed arms than their respective wild-type littermates. HdhQ350/+ (C) males and (D) females spent similar amounts of time in the open arms than their respective wild-type littermates. Exploration was measured by the distance mice traveled within the first hour of being placed into the PhenoTyper chamber. (E) Male HdhQ350/+ mice and (F) female HdhQ350/+ mice covered similar distances than their respective wild-type littermates at 40 and 60 weeks of age. N=7–8 for all groups. Error bars represent S.E.M., with two-way ANOVA with Bonferroni post-hoc test.

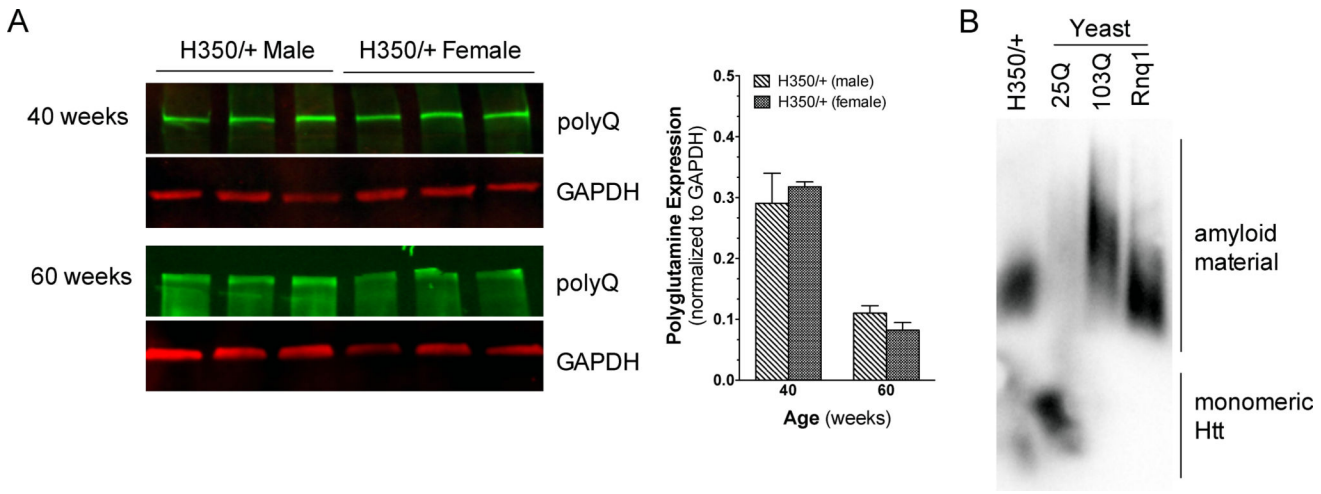

Figure 7. mHtt expression and aggregation in striatal tissue of HdhQ350/+ males and females

Western blot of polyglutamine expansion at 40 and 60 weeks of age in (A) male and female HdhQ350/+ mice. Quantification of mHtt between male and female HdhQ350/+ mice showed no difference in protein expression levels. (B) SDDAGE blot comparing SDS solubility of striatal H350/+ tissue to yeast strains of 25 polyglutamines, 103 polyglutamines and prion Rnq1. Error bars represent S.E.M., with two-way ANOVA with Bonferroni post-hoc test.

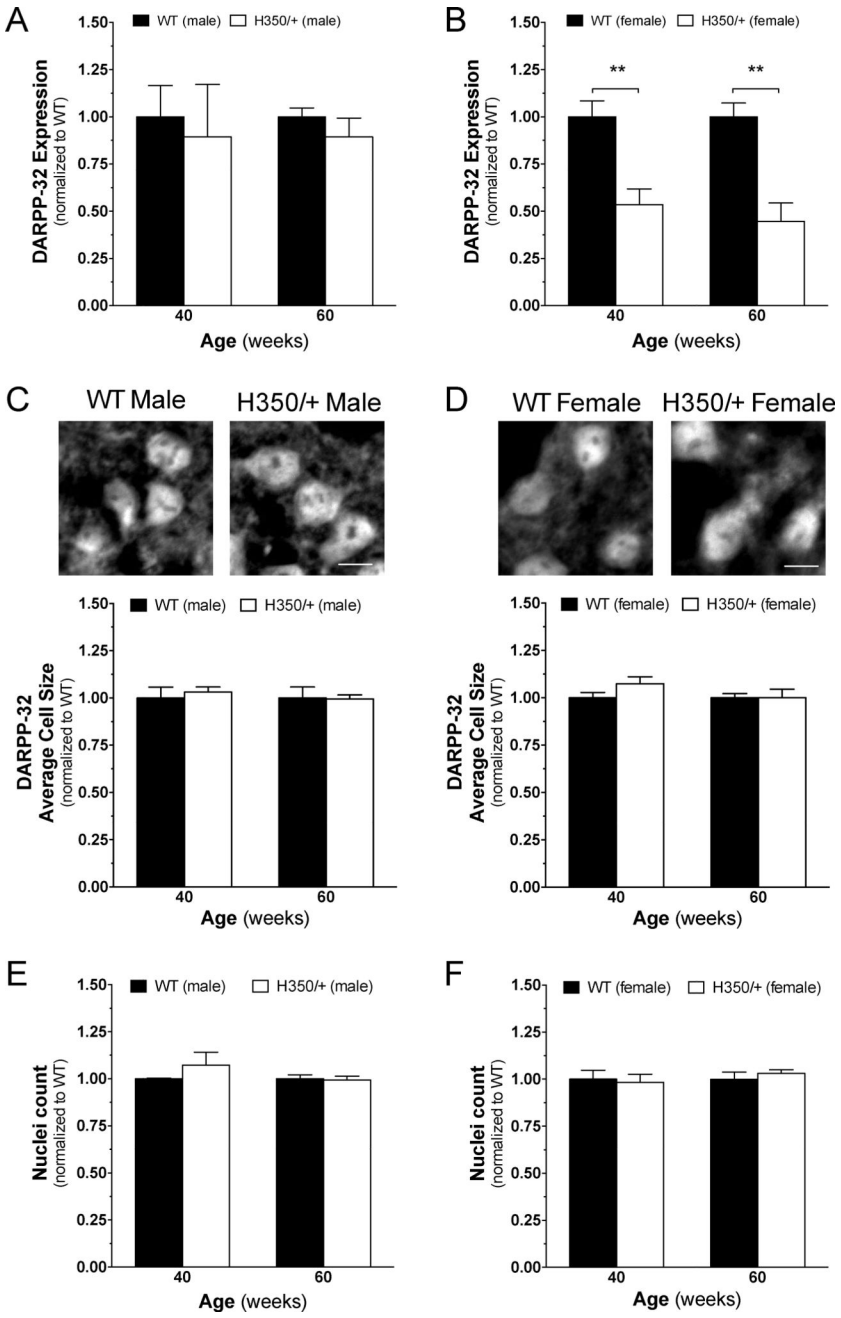

Figure 8. HdhQ350/+ females, but not males, exhibit typical HD protein loss in the striatum

(A) Male HdhQ350/+ mice did not show changes in DARPP-32 protein expression at 40 or 60 weeks when compared to male wild-type littermates. (B) Female HdhQ350/+ mice showed significant reductions in DARPP-32 protein expression at 40 and 60 weeks of age. (C) Male HdhQ350/+ and (D) female HdhQ350/+ mice had no significant differences in average size of DARPP-32-positive cells compared to respective wild-type littermates. Representative images are cropped and captured at 40×. Scale bar denotes 10um. DAPI-positive cells quantified in the dorsolateral striatum showed no difference in (E) male HdhQ350/+ and (F) female HdhQ350/+ mice when compared to their respective wild-type

littermates. N=3 for all groups. Error bars represent S.E.M. and **p<0.01, with two-way ANOVA with Bonferroni post-hoc test.